EUR Research Information Portal

Lower fractional anisotropy without evidence for neuro-inflammation in patients with early-phase schizophrenia spectrum disorders

Published in:
Schizophrenia Research

Publication status and date:
Published: 01/02/2024

DOI (link to publisher):
10.1016/j.schres.2022.12.009

Document Version
Version created as part of publication process; publisher's layout; not normally made publicly available

Document License/Available under:
CC BY

Erasmus University Rotterdam
Making Minds Matter

Lower fractional anisotropy without evidence for neuro-inflammation in patients with early-phase schizophrenia spectrum disorders

Shiral S. Gangadin [a,*], René C.W. Mandl [a], Lot D. de Witte [b], Neeltje E.M. van Haren [c], Maya J.L. Schutte [a], Marieke J.H. Begemann [a], René S. Kahn [b], Iris E.C. Sommer [a]

[a] Section Cognitive Neuroscience, Department of Biomedical Sciences of Cells & Systems, University Medical Center Groningen, University of Groningen, Groningen, the Netherlands
[b] Department of Psychiatry, Icahn School of Medicine at Mount Sinai, New York City, NY, USA
[c] Department of Child and Adolescent Psychiatry/Psychology, Erasmus University Medical Center-Sophia Children's Hospital, Rotterdam, the Netherlands

ARTICLE INFO

ABSTRACT

Various lines of research suggest immune dysregulation as a potential therapeutic target for negative and cognitive symptoms in schizophrenia spectrum disorders (SSD). Immune dysregulation would lead to higher extracellular free-water (EFW) in cerebral white matter (WM), which may partially underlie the frequently reported lower fractional anisotropy (FA) in SSD. We aim to investigate differences in EFW concentrations – a presumed proxy for neuro-inflammation – between early-phase SSD patients ($n = 55$) and healthy controls (HC; $n = 37$), and to explore immunological and cognitive correlates. To increase specificity for EFW, we study several complementary magnetic resonance imaging contrasts that are sensitive to EFW. FA, mean diffusivity (MD), magnetization transfer ratio (MTR), myelin water fraction (MWF) and quantitative T1 and T2 were calculated from diffusion-weighted imaging (DWI), magnetization transfer imaging (MTI) and multicomponent driven equilibrium single-pulse observation of T1/T2 (mcDESPOT). For each measure, WM skeletons were constructed with tract-based spatial statistics. Multivariate SSD-HC comparisons with WM skeletons and their average values (i.e. global WM) were not statistically significant. In voxel-wise analyses, FA was significantly lower in SSD in the genu of the corpus callosum and in the left superior longitudinal fasciculus ($p < 0.04$). Global WM measures did not correlate with immunological markers (i.e. IL1-RA, IL-6, IL-8, IL-10 and CRP) or cognition in HC and SSD after corrections for multiple comparisons. We confirmed lower FA in early-phase SSD patients. However, non—FA measures did not provide additional evidence for immune dysregulation or for higher EFW as the primary mechanism underlying the reported lower FA values in SSD.

1. Introduction

The inability of antipsychotics to relieve all symptom domains of schizophrenia spectrum disorders (SSD; i.e. schizophrenia, schizo-affective disorder, schizophreniform disorder and psychosis not otherwise specified), has driven research to explore other biological pathways. New therapeutic options for the negative (e.g. blunted affect) and cognitive (e.g. reduced processing speed) symptom domains are urgently needed. Various lines of research suggest a role for neuro-inflammation, or rather immune dysregulation, early in the development of SSD (Fond et al., 2020).

A dysregulated immune system entails subtle signs of immune

involvement, such as aberrant activation of microglia (i.e. the resident immune cells of the central nervous system) (Trépanier et al., 2016; van Kesteren et al., 2017), increased levels of pro-inflammatory cytokines (Frydecka et al., 2018) and increased extracellular free water (EFW) (Brocker et al., 2012). The latter may be specifically affecting the brain's white matter (WM) (Dietz et al., 2020; Najjar and Pearlman, 2015). Free water refers to unrestricted water molecules that move freely in any direction. EFW is thus free water in extracellular spaces, such as interstitial fluid, cerebrospinal fluid (CSF) and blood plasma (Pasternak et al., 2016). Increased EFW in WM is a presumed proxy of immune dysregulation, assuming that immune dysregulation manifests in interstitial fluid accumulation. This interstitial EFW increase might be a result of

neuro-inflammatory processes (i.e. low grade cerebral edema due to blood-brain barrier hyper-permeability or microglial activation) (Dalby et al., 2021; Pollak et al., 2018), yet several other factors influence EFW as well (e.g. atrophy, decreased cellularity and synaptic pruning) (Guo et al., 2020).

The immunological deviations in SSD are small and the evidence for this immune hypothesis is not consistent (Birnbaum and Weinberger, 2020; Snijders et al., 2021). This includes conflicting evidence from positron emission tomography (PET) studies (Marques et al., 2019; Plavén-Sigray et al., 2021), which use tracers that do not seem to specifically reflect activated microglia in schizophrenia (Sneeboer et al., 2020). As post-mortem investigation and PET imaging both have considerable limitations, the use of non-invasive magnetic resonance imaging (MRI) has been proposed to measure the pro-inflammatory status of the brain (i.e. EFW) (Gangadin et al., 2019; Pasternak et al., 2016).

Several MRI contrasts are sensitive, albeit through different mechanisms, to EFW that *putatively* reflects immune dysregulation (Gangadin et al., 2019; Harrison et al., 2015; Pasternak et al., 2016). Diffusion-weighted MRI (DWI), for example, can be used to obtain information of the diffusion profile of water molecules. Tensor-derived scalar measures include fractional anisotropy (FA) and mean diffusivity (MD). FA describes directional differences in diffusion rate and is often used as a proxy for microstructural organisation and MD describes mean diffusion rate. These measures can be computed to study the microstructure of the brain's WM. In WM, water moves more easily in a direction parallel to the axons than in a perpendicular direction, leading to relatively high FA values. When EFW increases, the isotropic diffusion component increases leading to lower FA and higher MD. Widespread lower FA in SSD has frequently been reported (Kelly et al., 2018; Wheeler and Voineskos, 2014). However, interpretation is difficult, as FA and MD are not only sensitive to EFW concentration but also to level of myelination, axonal diameter, packing density and alignment of the axons.

To improve specificity of DWI, recent studies adjusted the tensor modelling to derive a component more sensitive to EFW than FA. This method demonstrated group-level increases of EFW, especially in patients with early-phase SSD compared to healthy controls (HC) (Chang et al., 2021; Guo et al., 2020; Lyall et al., 2017; Pasternak et al., 2012). In chronically ill patients, EFW increases were not observed (Gurholt et al., 2020; Oestreich et al., 2017). The hypothesis that EFW increases are associated with immune dysregulation is supported by DWI studies that find significant correlations with clinical markers of inflammation (i.e. peripheral cytokines and glutathione levels in brain) (Di Biase et al., 2021; Lesh et al., 2019; Rodrigue et al., 2019). Recent preclinical studies also demonstrated increased EFW in WM after immune activation (i.e. maternal immune activation and interferon-γ overexpression) (Di Biase et al., 2020; Febo et al., 2020). Although this line of research is incipient, immune dysregulation – presumably reflected in EFW increases – is hypothesized to occur during the early phase of SSD, whereas WM tissue degeneration (i.e. atrophy or demyelination) might be more characteristic for the chronic phase (Gangadin et al., 2019; Pasternak et al., 2016).

To increase specificity for EFW, DWI can also be combined with other MRI contrasts, such as magnetization transfer imaging (MTI) (Kubicki et al., 2005; Mandl et al., 2015) or myelin water imaging (Lipp et al., 2019). These methods are sensitive to water in the extracellular space, but with multiple other interpretations. However, these three methods are complimentary and studying them collectively could provide additional information on EFW in SSD.

With MTI, an excitation pulse is exclusively targeted at macromolecules, including myelin. The magnetization then partially transfers to the free water pool. The magnetization transfer ratio (MTR) can be computed between images with and without an excitation pulse. The MTR is considered a proxy of myelin concentration. MTR is also sensitive to EFW, as the amount of transfer depends on both the concentration of macromolecules and on the concentration of extracellular water. With myelin water imaging it is possible, using a series of T2 measurements, to

determine the fraction of water that is trapped between the myelin's lipid bilayers, which is characterized by a very short T2 relaxation time. This myelin water fraction (MWF) is considered to be a more specific marker for myelin concentration (Kolind et al., 2009; MacKay and Laule, 2016). Myelin water imaging not only allows to compute the MWF but can also provide quantitative T1 (qT1) and T2 (qT2) measures that are sensitive to EFW. Previous studies yielded heterogeneous results regarding group differences in MWF (i.e. SSD vs. HC) and correlations with cognitive performance (Flynn et al., 2003; Lang et al., 2014; Vanes et al., 2018, 2019).

Given the added value of multimodal MRI, this study sets out to investigate reflections of EFW in early-phase SSD and controls using several complementary MRI contrasts. We aim to explore differences in EFW between early-phase SSD patients and HC. Higher EFW concentrations in the WM in patients with SSD relative to HC would be reflected in a lower FA and higher MD, MTR and quantitative T1 and T2. We expect to find no differences in MWF between groups. Finally, we explore correlations between these MRI measures with immunological markers, cognitive performance and clinical measures to provide new insight into the biology of SSD.

2. Methods

2.1. Participants

Table 1 shows demographical and clinical characteristics of all participants with SSD ($n = 55$) and HC ($n = 37$). Participants in the SSD group were eligible for study inclusion when aged between 18 and 50, diagnosed with schizophrenia, schizoaffective, schizophreniform disorder (295.x) or psychotic disorder not otherwise specified (298.9) within 3 years prior to screening. Participants in the HC group were excluded when they had a family history with psychiatric illness (i.e. parents or siblings). Participants from both studies were excluded in case of MRI contra-indications (i.e. claustrophobia or ferrous implants or medical devices). The Positive and Negative Syndrome scale (PANSS) and the Brief Assessment of Cognition in Schizophrenia (BACS) were used to assess symptom severity and cognition (Kay et al., 1987; Keefe et al., 2004). Other exclusion criteria and a full description or procedures were published previously (Begemann et al., 2015). Although 119 participants of in the trial (Sommer et al., 2021) were invited to have MRI scans, not all accepted the invitation. A full set of MRI scans (i.e. DTI, MTR, and mcDESPOT) was performed for 60 participants at baseline. In addition 5 scans were excluded from the analyses (2 scans did not include the entire brain inside the field of view and the MTR signal was outside reasonable ranges in 3 scans).

Blood was drawn in the morning of the baseline visit. We analysed the levels of a panel of inflammatory markers that have been associated with schizophrenia in recent meta-analyses (de Witte et al., 2014; Frydecka et al., 2018; Goldsmith et al., 2016; Wang et al., 2017). High-sensitivity C-reactive protein (CRP) was measured in these samples through the central diagnostic laboratory of the UMC Utrecht and Groningen using the Siemens Atellica™ Solution turbidimetric immunoassay. In addition, serum was prepared and stored at-80 °C in aliquots within 4 h after blood draw by the Central Biobank of the UMC Utrecht. At the end of the study, Interleukin (IL)-6, IL-8, IL-10, IL-1 Receptor Agonist (IL-1RA) were assessed using the Meso Scale Discovery U-PLEX Assay Platform (MSD Cat #K15067M, customized) and S-PLEX Human IL-6 Kit (MSD Cat# K151B3S), according to the manufacturer's protocol. All samples were detected within the standard range of the assay.

MRI acquisition and participant recruitment from Dutch mental healthcare settings were part of the Simvastatin and the Controls trial. These trials were approved by the research and ethics committee of the University Medical Center Utrecht (UMCU), the Netherlands, under protocol numbers: 13–249 and 14–572, respectively (Simvastatin trial registration: ClinicalTrails.gov:NCT01999309; EudraCT-number:2013 –000834-36. Controls trial registration: ABR NL50657.041.14). These

Table 1

Demographic and clinical characteristics of the participants. Ranges are displayed between brackets. BACS: Brief Assessment of Cognition in Schizophrenia; IQR: interquartile range; PANSS: Positive and Negative Syndrome Scale; pg: picogram; SD: standard deviation; W: Wilcoxon test statistic.

	SSD (n = 55)	HC (n = 37)	Statistics
Age, mean (SD), y	27.9 (6.6) [18–50]	24.5 (5.1) [19–43]	$t(87.9) = 2.81$, $p = 0.006$
Sex, F/M	15/40	7/30	$X^2(1) = 0.45$, $p = 0.502$
Education mean (SD), y	13.5 (2.4) [6–17]	15.0 (2.0) [10–17]	$t(84.8) = -3.26$, $p = 0.002$
Diagnosis, n (%)			
Psychosis not otherwise specified (298.9)	31 (56.4)	–	
Schizophrenia (295.x)	19 (34.5)	–	
Schizoaffective disorder (295.70)	4 (7.3)	–	
Schizophreniform disorder (295.40)	1 (1.8)	–	
Duration of illness, mean (SD), y	1.0 (0.9) [0–3]	–	
Antipsychotic dose, mean (SD), chlorpromazine equivalent	310.6 (243.9) [0–900]	–	
PANSS total score, mean (SD)	56.8 (12.9) [33–85]	–	
PANSS Positive subscale, mean (SD)	12.7 (4.3) [7–28]	–	
PANSS Negative subscale, mean (SD)	15.0 (5.3) [7–28]	–	
PANSS General subscale, mean (SD)	29.1 (6.1) [17–45]	–	
BACS composite, standardized mean (SD)	−1.2 (1.3) [−3.4–2.3]	0.1 (1.2) [−3.2–2.0]	$t(80.2) = -5.16$, $p = 1.7 \times 10^{-6}$
Interleukin-10, median (IQR), pg/mL	0.20 (0.16) [0.04–0.96]	0.17 (0.12) [0.03–1.01]	$W = 1163$, $p = 0.248$
Interleukin-1 Receptor Antagonist, median (IQR), pg/mL	270 (161) [126–953]	270 (152) [116–636]	$W = 1030$, $p = 0.923$
Interleukin-6, median (IQR), fg/mL	493 (368) [225–1273]	390 (344) [123–2581]	$W = 1204$, $p = 0.139$
Interleukin-8, median (IQR), pg/mL	8.62 (3.49) [3.39–20.3]	7.10 (3.13) [2.82–24.1]	$W = 1243$, $p = 0.073$
C-Reactive Protein, median (IQR), mg/L	1.3 (1.9) [0.2–12]	1.1 (2.4) [0.4–35]	$W = 1003.5$, $p = 0.914$
MRI scanner, scanner 1/ scanner 2	17/38	10/27	$X^2(1) = 0.03$, $p = 0.867$

studies were conducted in compliance with the Declaration of Helsinki (2013). All participants provided written informed consent prior to participation.

2.2. MRI acquisition

MRI data were acquired on a Philips Achieva 3.0 T scanner using an 8-channel SENSE head coil at the UMCU from March 2015 till October 2015, after which the scanner was replaced and a system upgrade was implemented. From April 2016 till February 2019 a Philips Ingenia 3.0 T CX (software version R530) and a 32-channel SENSE head-coil were used. The following sequences were acquired: a double turbo spin echo T2-weighted sequence (TE/TR = 3.4/6000 ms, flip angle = 90°, 120 slices, slice gap = 0 mm, acquired voxel size = $1 \times 1.25 \times 1.6mm^3$, FOV = 256x204x192mm^3), two diffusion-weighted echo-planar imaging sequences (identical except for k-space readout direction = anterior vs. posterior, TE/TR = 69/7110 ms, flip angle = 90°, 75 slices, slice gap = 0 mm, acquired voxel size = $1.88 \times 2.35 \times 2mm^3$, FOV = 240x240x150mm^3, b-value = 1000 s/mm^2 for 30 volumes and b = 0 s/mm^2 for five volumes), a 3D fast field echo magnetization transfer sequence (TE/TR = 2.3/56 ms, flip angle = 18°, 95 slices, acquired voxel

size = 1.88x1.88x4mm^3, FOV = 240x180x190mm^3, off-resonance pre-pulse = 1100 Hz; 620°; three-lobe sync shaped and the multicomponent driven equilibrium single-pulse observation of T1/T2 (mcDESPOT) protocol (acquired voxel size = 1.7 mm isotropic, FOV = 217x217x156mm^3, 92 slices). This protocol consisted of balanced steady-state free precession (bSSFP; TE/TR = 2.9/5.8 ms, flip angles = [7,10,11,15,19,24,30,47]), Spoiled gradient recalled echo (SPGR; TE/TR = 3.6/6.5 ms, flip angles = [2,3,4,5,6,9,13,18], radio-frequency phase cycling pattern of 0° and 180°) and inversion recovery SPGR (IR-SPGR; TE/TR = 3.2/6.5 ms, flip angle = 5) sequences (Deoni et al., 2008).

2.3. Pre-processing

DWI processing and analysis was performed using the using Oxford Centre for Functional MRI of the Brain (FMRIB) Software Library version 6.0.1. (FSL; http://www.fmrib.ox.ac.uk/fsl) and the MRtrix toolbox (http://www.mrtrix.org). Processing included noise filtering (denoising and Gibbs ringing removal; MRTrix), correction for susceptibility-induced distortion head motion effects, correction for eddy currents (including quality assessment), and finally tensor fitting (FMRIB Diffusion Toolbox; FDT).

Magnetization transfer imaging resulted in two images, one with magnetization pre-pulse (I_m) and one image without (I_0). The MTR was calculated with the following equation MTR = ($I_0 - I_m$)/ I_0. In native space, the MTR images were skull-stripped (FSL's Brain extraction Tool; BET) (Smith, 2002) and the I_0 image was linearly registered to the diffusion unweighted (b = 0 s/mm^2) volume of the DWI scan (FMRIB's Linear Image Registration Tool; FLIRT) (Jenkinson et al., 2002). Mutual information was used as similarity metric for registration.

The scans from the mcDESPOT protocol were processed using Quantitative Imaging Tools (QUIT) software (Wood, 2018). Brain extraction (BET) and resampling was used to calculate a brain mask from the T2 weighted image. Next, quantitative T1 (qT1), B1 (Deoni, 2007), quantitative T2 (qT2) and off-resonance maps (Deoni, 2009) were calculated from the data. Lastly, MWF maps were calculated using a 3 component model (Deoni et al., 2013) and Gaussian Region Contraction (Deoni and Kolind, 2015). The qT1, qT2 and MWF maps were also linearly registered to the B0 volume (FLIRT).

Voxel-based analysis was performed using tract-based spatial statistics (TBSS) (Smith et al., 2006) according to the ENIGMA-TBSS protocol (http://enigma.ini.usc.edu/protocols/dti-protocols/). In short, for the DWI data a single tensor model was fitted after which FA (and MD) maps were computed for each subject. Next, the FA maps (in native space) were nonlinearly registered to the ENIGMA-FA model after which the registered FA maps were projected onto the ENIGMA-DTI template skeleton, resulting in an FA skeleton for each subject. The same transformations computed for the FA maps were applied to the non-FA measures (MD, MTR, MWF, qT1 and qT2), after they were registered to the B0 map from the DWI data. Global values for these measures were computed by averaging over all skeleton voxels. Fig. 1 shows the processing pipeline.

2.4. Statistical analysis

To explore the group differences in global (i.e. mean white matter skeleton) MRI measures, a multivariate analysis of variance (MANOVA) was performed, using R version 3.6.1. This MANOVA was followed by six ANOVA's for each MRI measure (FA, MD, MTR, MWF, qT1 and qT2). To explore these group differences on voxel-level, Permutation Analysis for Linear Models (Winkler et al., 2014) was used. This program is based on the randomise program in FSL (Winkler et al., 2014). The voxel-wise MANOVA was also followed by six voxel-wise ANOVAs. All voxel-wise tests were performed two-sided, with 10.000 permutations, threshold-free cluster enhancement (TFCE) and family-wise error (FWE) correction, using randomise. The multivariate analyses used Pillai's trace as
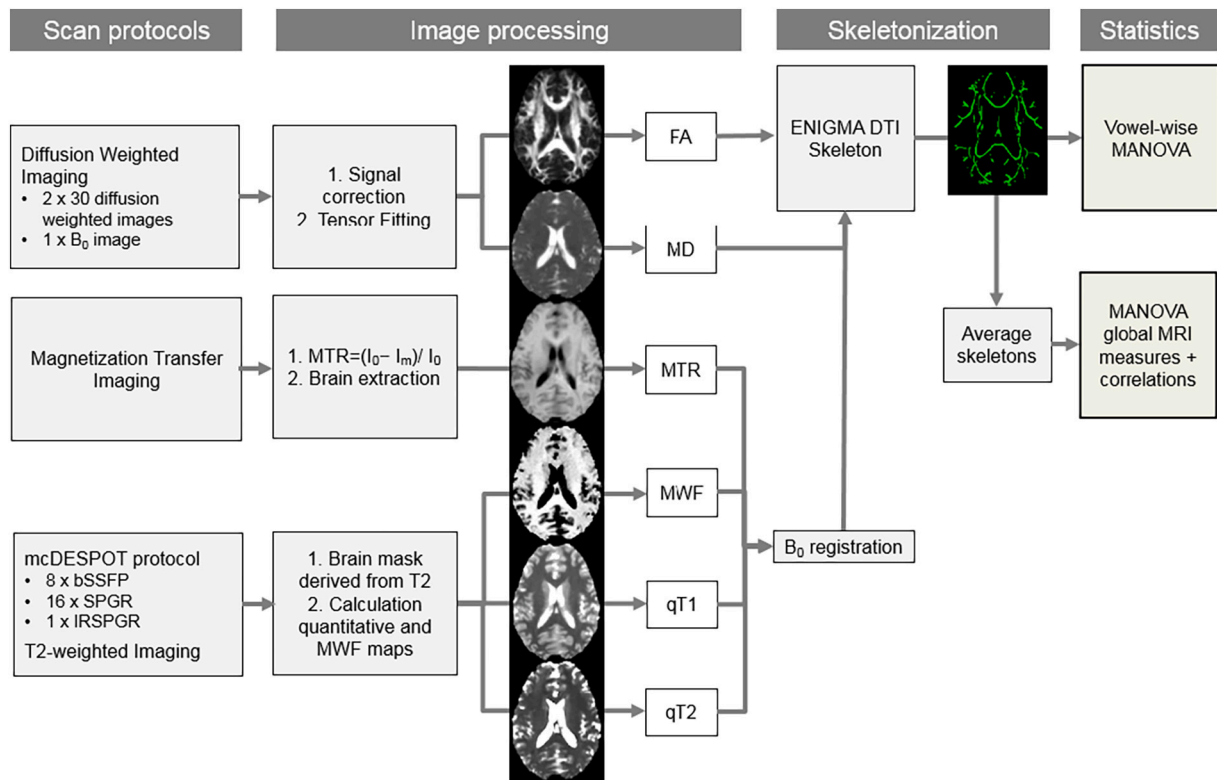
Fig. 1. MRI processing procedures. Processing the images from the three different scan protocols, resulted in six different MRI maps. These maps were aligned and registered to the ENIGMA DTI FA skeleton, after which statistics were performed on the average skeleton values and on voxel-level. bSSFP: balanced steady-state free precession; DTI: diffusion tensor imaging; FA: fractional anisotropy; IR-SPGR: inversion recovery spoiled gradient recalled echo; MANOVA: multivariate analysis of variance; mcDESPOT: multicomponent driven equilibrium single-pulse observation of T1/T2; MD: mean diffusivity; MTR: magnetization transfer ration; MWF: myelin water fraction; SPGR: spoiled gradient recalled echo; qT1: quantitative T1; qT2: quantitative T2.

multivariate test statistic and all analyses included age, sex, handedness and scanner as covariates. As age is higher in SSD relative to HC (Table 1), we corrected for age by adding it to the MANOVA for global effects and to the voxel-wise analyses as a centered continuous variable. Scanner was added to these analyses as a dichotomous variable, indicating whether the participant was scanned at the first or the second scanner (see Supplementary Fig. S1 for the global MRI measures per individual across the scanners). The level of statistical significance was set at 0.05 for all multivariate analyses.

For HC and SSD separately, correlation coefficients were calculated between global MRI measures and symptom severity, cognition, immune markers and immunological confounds (i.e. BMI and smoking) using Spearman correlations. Normal distribution of the variables was checked by visual inspection of histograms and q-q plots. All immunological variables were normally distributed after logarithmic transformation. Uncorrected p-values ($p < 0.05$) and Bonferroni corrected p-values ($p < 0.0001$) are reported for the correlation analyses, as these analyses are explorative in nature. Correlations between MRI measures and immune markers, cognition and the other MRI measures were statistically compared between HC and SSD with post-hoc regression analyses that included the interaction between the MRI measure and the group (i.e. global FA*Group). These analyses were corrected for age, sex, handedness, scanner, BMI and cigarette use.

3. Results

3.1. Group comparisons

Multivariate global group differences did not reach statistical significance (Pillai's Trace = 0.12, F(6, 80) =1.88, $p = 0.095$). Exploring individuals measures revealed that global FA differed between the

groups (F(1, 86) = 5.55, $p = 0.021$; Fig. 2A), although this does not remain significant after correcting for the six comparisons. The SSD group (0.44 ± 0.02) had a lower mean FA compared to HCs (0.45 ± 0.02). Figs. 2A-F show the distribution of all MRI measures per group. Table S1 shows the scanner*group effects as well as the results of the multivariate global group differences, with and without the scanner included as a covariate. No significant scanner*group interactions were found in the multivariate (F(6, 79) =0.23, $p = 0.96$) and univariate analyses of the six MRI measures ($p > 0.85$). As a result, the scanner variable without interaction was included as a covariate in the abovementioned final analyses.

Voxel-wise multivariate (Pillai's trace = 1017.6, FWE $p = 0.40$) and univariate (FWE $p > 0.05$) group comparisons did not reach statistical significance, except for FA (FWE $p = 0.016$). Again, SSD had lower FA than HC, predominantly in the genu of the corpus callosum and the left superior longitudinal fasciculus (SLF) (Fig. 3; Table S2). All immunological markers did not show a significant difference between the groups ($p > 0.05$; Table 1).

3.2. Correlations

Fig. 4 shows the correlation matrices between global MRI measures and several clinical and immunological variables for HC and SSD separately. In both groups, FA and MD (HC: $r = -0.61, p = 7.15 \times 10^{-5}$; SSD: $r = -0.70, p = 2.37 \times 10^{-9}$) and MWF and qT1 (HC: $r = -0.68, p = 4.51 \times 10^{-6}$; SSD: $r = -0.78, p = 3.46 \times 10^{-12}$) showed statistically significant correlations. No significant correlations between immunological markers or cognition and MRI measures were found in both groups.

When evaluating the correlation results at the threshold of $p < 0.05$, it is interesting to note that the HC group shows more correlations between MRI measures with both immune markers and cognition
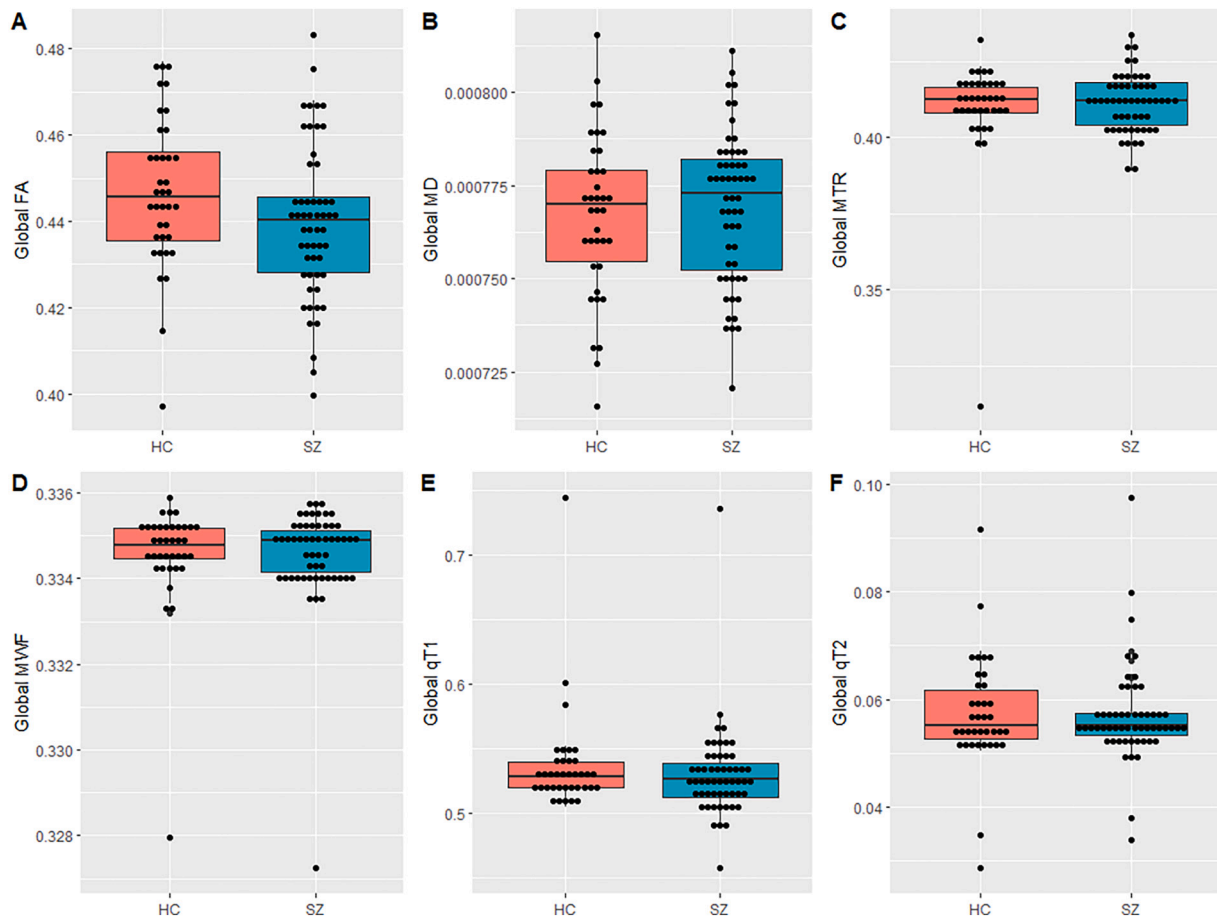
Fig. 2. Distribution of global MRI measures per group. Group differences in global: A, fractional anisotropy (FA); B, mean diffusivity (MD); C, magnetization transfer ration (MTR); D, myelin water fraction (MWF); E, quantitative T1 (qT1); F, quantitative T2 (qT2). HC: healthy controls; SSD: schizophrenia spectrum disorder.

compared with SSD patients. For example, in SSD only IL1-RA was positively related to MD ($r = 0.38$, $p = 0.0042$) whereas in HC IL-8 was related to both FA ($r = -0.34$, $p = 0.041$) and qT1 ($r = 0.42$, $p = 0.011$) and CRP to MTR ($r = 0.40$, $p = 0.015$). In addition, FA is related to motor speed ($r = 0.36$, $p = 0.032$), executive functioning (Tower of London; $r = 0.47$, $p = 0.003$) and the total cognition score ($r = 0.42$, $p = 0.012$) in HC, but not to any cognitive score in SSD.

However, regression analyses show no differences in the correlations between the MRI measures and immune markers, cognition and the other MRI measures, between the two groups after corrections for multiple testing and covariates (Table S3). Only the relation between motor speed and MTR shows a trend-level difference between groups (B = 43.0, $p = 0.029$). The HC group shows negative association (B = -11.38, $p = 0.262$) and the SSD group shows a positive association between motor speed and MTR (B = 31.65, $p = 0.072$).

No significant effects were found for the group differences in MRI measures and immune markers or for the correlation between these variables in the SSD or in HC group, using partial least squares correlation analyses (methodology and results described in Supporting Information).

4. Discussion

In this study, we aimed to explore differences in EFW between patients with early-phase SSD and HC and to identify the immunological, cognitive and clinical correlates of EFW. EFW was probed through several proxy measures: FA, MD, MTR, MWF, qT1 and qT2. Only differences between SSD and HC in FA were confirmed on voxel-level, but no other significant differences or correlations were found. FA

differences were significant in the genu of the corpus callosum and the left SLF.

4.1. No evidence of immune dysregulation in WM

Higher EFW was hypothesized to be reflected in lower FA, and higher MD, MTR, qT1 and qT2. The lack of significant non-FA group differences may suggest the absence of increased EFW in this early stage SSD sample (mean illness duration: 1y). In addition, SSD patients did not demonstrate elevated levels of peripheral immune markers relative to HC, which could suggest the absence of immune dysregulation. A recent meta-analysis on DWI studies did reveal significantly higher EFW in SSD patients (Carreira Figueiredo et al., 2022), an effect that was mainly driven by two first episode psychosis samples (Lyall et al., 2017; Pasternak et al., 2012). Yet, results from non-DWI studies in early-phase SSD do not support that hypothesis (Guo et al., 2020; Kraguljac et al., 2019; Lang et al., 2014; Mandl et al., 2015), nor does the current study. These studies consistently refer to short duration of illness and young age as possible explanations for the absence of group effects, which are also relevant explanations for our findings. Illness duration was related to microstructural WM measures in other studies (Kraguljac et al., 2020), but the strong correlation between illness duration and age makes it hard to differentiate both effects (Kelly et al., 2018).

Low FA in the genu of the corpus callosum (Shahab et al., 2018) and the left SLF (Zhou et al., 2017) was previously demonstrated for early-phase SSD patients. Associative WM tracts that connect higher-order brain areas (e.g. corpus callosum) mature later in life and show more pronounced SSD-HC differences (Kochunov et al., 2016). This could also explain the lower FA values in the corpus callosum observed in this
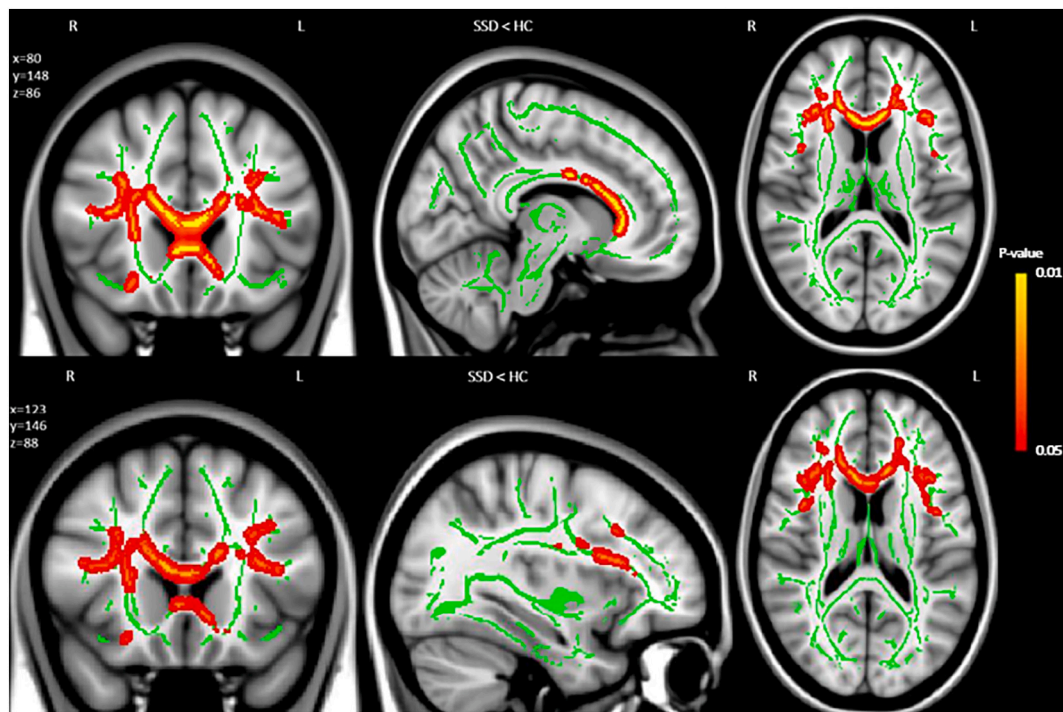
Fig. 3. Significant voxels from the tract-based spatial statistics (TBSS) analysis showing decreased FA in schizophrenia spectrum disorder (SSD) compared with healthy control (HC) subjects (family-wise error corrected $p = 0.016$) in the genu of the corpus callosum (above) and the left superior longitudinal fasciculus (SLF) (below). On the MNI152 standard space T1 image (grayscale), the ENIGMA FA skeleton (green) and significant TBSS voxels (red-yellow; SSD < HC, corrected $p < 0.05$) were projected. Coordinates corresponding to the centre of gravity of the largest cluster (genu: x = 80, y = 148, z = 86; SLF: x = 123, y = 146, z = 88). (For interpretation of the references to colour in this figure legend, the reader is referred to the web version of this article.)
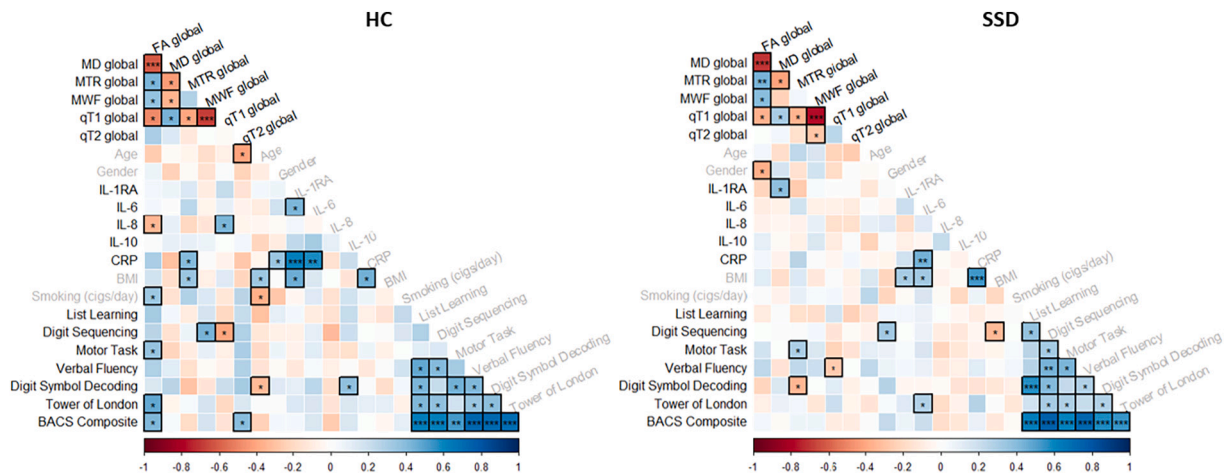

Fig. 4. Correlations between MRI measures, demographics (age and gender), immunological parameters and confounds (BMI and smoking), and cognitive performance in healthy controls (HC; left) and in patients with schizophrenia spectrum disorder (SSD; right). Correlations of the variables in black were compared between the two groups in later analyses. The colour of an individual matrix element represents the correlation strength (r) between −1 and 1. Black rectangles indicate p < 0.05, * p < 0.05, ** $p < 0.001$, *** $p < 0.0001$ (Bonferroni correction).

study.

4.2. Clinical and immunological correlates of WM microstructure

A recent article showed an association between EFW in SSD and peripheral IL-6 and tumour necrosis factor α, while other interleukins did not (Di Biase et al., 2021). In our explorative analyses, we found a trend-level correlation between MD and IL1-RA in SSD, but not between other MRI measures and immunological markers (IL-6, IL-8, IL-10, CRP). IL1-RA protein levels previously showed elevations in SSD (Frydecka

et al., 2018). Our results suggest that IL-1-related pathways might be associated with WM microstructure.

No statistically significant correlations between MRI measures and cognitive functions were found. HC showed more associations between global MRI measures and cognition than controls, especially in global FA. Previous studies also reported correlations between WM microstructure (i.e. MWF, FA, MTR) and cognition in controls, which were absent in SSD patients (Erkol et al., 2020; Lang et al., 2014; Nazeri et al., 2013). In addition, a recent study with early-phase SSD participants also found no associations between cognition an EFW (Hegde et al., 2020). It

may be possible that cognitive function is more related to the microstructure of the tissue itself (i.e. FA), rather than EFW surrounding the tissue.

4.3. Immune dysregulation and other factors affecting WM structure

Alterations in WM microstructure may arise from processes other than increased EFW (i.e. immune dysregulation) as well. Immune dysregulation in SSD is yet not well-understood. For example, microglia pathology in SSD seems more complex than activation versus inactivation (Snijders et al., 2021). In addition, early promising results from clinical trials with anti-inflammatory agents (Çakici et al., 2019), could not be replicated in recent studies with more subjects (Jeppesen et al., 2020; Sommer et al., 2021; Weiser et al., 2020).

Lower FA in SSD could also be explained by aberrant organisation of the WM (e.g. axonal organisation, myelination) or other pathophysiological mechanisms. A normalizing effect of antipsychotics cannot be excluded without MRI scans before initiation of medication in this study. Antipsychotics have been shown to decrease cytokine levels and FA (Çakici et al., 2021; Szeszko et al., 2014). However, EFW was found to be unaffected by risperidone treatment (Kraguljac et al., 2019). Interestingly, FA decreases after antipsychotic medication were significantly related to low density lipoprotein (Szeszko et al., 2014). Other metabolic factors that are often elevated in SSD, such as obesity and cholesterol have been related to decreased FA as well (Hidese et al., 2020; Spangaro et al., 2018).

4.4. Limitations

As previously stated, the young age and short duration of illness of our study population may explain the lack of significant non-FA group differences, but certain methodological considerations have to be taken into account as well. First, our sample size may be considered modest for MRI studies, although it is comparable to recent multimodal MWF studies ($40 < n < 57$) that did report significant results (Bangen et al., 2021; Faizy et al., 2020). Second, although without statistical significance, the female:male ratio was higher in SSD than in HC. However, females with SSD show lower FA and higher MD in WM compared with male patients (Shahab et al., 2018). A better sex-matched sample with less female patients would therefore actually decrease our effect size. Third, our findings may not be explained by the age difference between groups, since we corrected for age in our analyses. In addition, older SSD patients are likely to demonstrate more immune dysregulation than younger HCs, as age is generally also related to innate immune activity (Godbout and Johnson, 2009). While peripheral cytokine levels do reflect immune dysregulation, central immunological markers would have been more specific for neuro-inflammation. Lastly, the 3.0 T MRI scanner was replaced for a newer version during the course of the trial. The SSD and HC participants were balanced over the two scanners (see fig. S1) and we applied a statistical correction for the replacement of the MRI scanner (Table S1), but this correction may not have removed all effects of the replacement. The use of different scanners may have increased variance. However, despite a potential increased variance, we were able to detect significant group differences in FA as well as correlations between interdependent MRI-derived global measures (i.e. MWF and qT1).

5. Conclusions

This multimodal study revealed FA reductions in SSD relative to HC, but no significant associations between MRI measures and both immunological markers and cognition. Group differences in other MRI measures and peripheral immunological markers were absent. These results provide no direct evidence for immune dysregulation in SSD nor for higher EFW as the primary mechanism underlying frequently reported lower FA in SSD. Other microstructural properties of WM, such as axonal

organisation may be underlying low FA in SSD instead. Future studies may benefit from including specific subgroups of patients with immune dysregulation and multimodal assessments could be used to further explore EFW as an immune proxy.

Ethics approval statement (also included in manuscript)

MRI acquisition and participant recruitment from Dutch mental healthcare settings were part of the Simvastatin and the Controls trial. These trials were approved by the research and ethics committee of the University Medical Center Utrecht (UMCU), the Netherlands, under protocol numbers: 13–249 and 14–572, respectively. These studies were conducted in compliance with the Declaration of Helsinki (2013).

Clinical trial registration (also included in manuscript)

Simvastatin trial registration: ClinicalTrails.gov:NCT01999309; EudraCT-number:2013–000834-36.

Patient consent statement (also included in manuscript)

All participants provided written informed consent prior to participation.

Permission to reproduce copyrighted material from other sources

No material is reproduced from other sources.

CRediT authorship contribution statement

Shiral S. Gangadin: Validation, Formal analysis, Investigation, Data curation, Writing – original draft, Visualization, Project administration. **René C.W. Mandl:** Methodology, Software, Formal analysis, Writing – original draft. **Lot D. de Witte:** Resources, Writing – review & editing. **Neeltje E.M. van Haren:** Resources, Writing – review & editing. **Maya J.L. Schutte:** Investigation, Writing – review & editing, Project administration. **Marieke J.H. Begemann:** Investigation, Writing – review & editing, Project administration. **René S. Kahn:** Conceptualization, Writing – review & editing, Funding acquisition. **Iris E.C. Sommer:** Conceptualization, Writing – review & editing, Supervision, Funding acquisition.

Declaration of competing interest

The authors declare no conflict of interest.

Data availability

The data that support the findings of this study are available on reasonable request from the corresponding author. The data are not publicly available due to privacy or ethical restrictions.

Acknowledgements

The authors thank all the participants of the study for their time and contribution. We thank the research assistants and interns for their support with the data collection. To this end, Jantina Brummelman, Sanne Schuite-Koops, Erna van 't Hag, Meike Bak, Margot Slot, Pascal Pas, Mascha Linszen, Sophie Heringa, Edwin van Dellen, Willemijn van der Veen, Lyliana Nasib and Bibi Navas Garcia, deserve a special mention. The following mental healthcare institutions were essential in our patient recruitment: UCP Groningen, Reinier van Arkel, Mentrum, UMC Utrecht, GGZ InGeest, GGZ Noord-Holland-Noord, Altrecht GGZ, GGZ Centraal. This work was supported by the Stanley Medical Research Institute (grant number: 12T-008) and the Dutch Research Council (NWO; grant number: 40-00812-98-12154). S.G. was supported by a Graduate School of Medical Sciences PhD scholarship from the University Medical Center Groningen (UMCG; Open Round 2018).

Appendix A. Supplementary data

Supplementary data to this article can be found online at https://doi. org/10.1016/j.schres.2022.12.009.

References

Bangen, K.J., Delano-Wood, L., Deoni, S.C.L., Clark, A.L., Evangelista, N.D., Hoffman, S. N., Sorg, S.F., Holmqvist, S., Osuna, J., Weigand, A.J., Jak, A.J., Bondi, M.W., Lamar, M., 2021. Decreased myelin content of the fornix predicts poorer memory performance beyond vascular risk, hippocampal volume, and fractional anisotropy in nondemented older adults. Brain Imaging Behav. https://doi.org/10.1007/s11682-021-00458-z.

Begemann, M.J.H., Schutte, M.J.L., Slot, M.I.E., Doorduin, J., Bakker, P.R., van Haren, N. E.M., Sommer, I.E.C., 2015. Simvastatin augmentation for recent-onset psychotic disorder: a study protocol. BBA Clin. 4, 52–58. https://doi.org/10.1016/j.bbacli.2015.06.007.

Birnbaum, R., Weinberger, D.R., 2020. A genetics perspective on the role of the (Neuro) Immune system in schizophrenia. Schizophr. Res. 217, 105–113. https://doi.org/10.1016/j.schres.2019.02.005.

Brocker, C., Thompson, D.C., Vasiliou, V., 2012. The role of hyperosmotic stress in inflammation and disease. Biomol. Concepts 3, 345–364. https://doi.org/10.1515/bmc-2012-0001.

Çakici, N., van Beveren, N.J.M., Judge-Hundal, G., Koola, M.M., Sommer, I.E.C., 2019. An update on the efficacy of anti-inflammatory agents for patients with schizophrenia: a meta-analysis. Psychol. Med. 49, 2307–2319. https://doi.org/10.1017/S0033291719001995.

Çakici, N., Sutterland, A.L., Penninx, B.W.J.H., de Haan, L., van Beveren, N.J.M., 2021. Changes in peripheral blood compounds following psychopharmacological treatment in drug-naïve first-episode patients with either schizophrenia or major depressive disorder: a meta-analysis. Psychol. Med. 1–12. https://doi.org/10.1017/S0033291721000155.

Carreira Figueiredo, I., Borgan, F., Pasternak, O., Turkheimer, F.E., Howes, O.D., 2022. White-matter free-water diffusion MRI in schizophrenia: a systematic review and meta-analysis. Neuropsychopharmacology 47 (7), 1413–1420.

Chang, X., Mandl, R.C.W., Pasternak, O., Brouwer, R.M., Cahn, W., Collin, G., 2021. Diffusion MRI derived free-water imaging measures in patients with schizophrenia and their non-psychotic siblings. Prog. Neuro-Psychopharmacol. Biol. Psychiatry 109, 110238. https://doi.org/10.1016/j.pnpbp.2020.110238.

Dalby, T., Wohl, E., Dinsmore, M., Unger, Z., Chowdhury, T., Venkatraghavan, L., 2021. Pathophysiology of cerebral Edema—a comprehensive review. J. Neuroanaesth. Crit. Care 08, 163–172. https://doi.org/10.1055/s-0040-1721165.

de Witte, L., Tomasik, J., Schwarz, E., Guest, P.C., Rahmoune, H., Kahn, R.S., Bahn, S., 2014. Cytokine alterations in first-episode schizophrenia patients before and after antipsychotic treatment. Schizophr. Res. 154, 23–29. https://doi.org/10.1016/j.schres.2014.02.005.

Deoni, S.C.L., 2007. High-resolution T1 mapping of the brain at 3T with driven equilibrium single pulse observation of T1 with high-speed incorporation of RF field inhomogeneities (DESPOT1-HIFI). J. Magn. Reson. Imaging 26, 1106–1111. https://doi.org/10.1002/jmri.21130.

Deoni, S.C.L., 2009. Transverse relaxation time (T 2) mapping in the brain with off-resonance correction using phase-cycled steady-state free precession imaging. J. Magn. Reson. Imaging 30, 411–417. https://doi.org/10.1002/jmri.21849.

Deoni, S.C.L., Kolind, S.H., 2015. Investigating the stability of mcDESPOT myelin water fraction values derived using a stochastic region contraction approach. Magn. Reson. Med. 73, 161–169. https://doi.org/10.1002/mrm.25108.

Deoni, S.C.L., Matthews, L., Kolind, S.H., 2013. One component? Two components? Three? The effect of including a nonexchanging "free" water component in multicomponent driven equilibrium single pulse observation of T 1 and T 2. Magn. Reson. Med. 70, 147–154. https://doi.org/10.1002/mrm.24429.

Deoni, S.C., Rutt, B.K., Arun, T., Pierpaoli, C., Jones, D.K., 2008. Gleaning multicomponent T1 and T2 information from steady-state imaging data. Magnetic Resonance in Medicine: An Official Journal of the International Society for Magnetic Resonance in Medicine 60 (6), 1372–1387.

Di Biase, M.A., Katabi, G., Piontkewitz, Y., Cetin-Karayumak, S., Weiner, I., Pasternak, O., 2020. Increased extracellular free-water in adult male rats following in utero exposure to maternal immune activation. Brain Behav. Immun. 83, 283–287. https://doi.org/10.1016/j.bbi.2019.09.010.

Di Biase, M.A., Zalesky, A., Cetin-Karayumak, S., Rathi, Y., Lv, J., Boerrigter, D., North, H., Tooney, P., Pantelis, C., Pasternak, O., Shannon Weickert, C., Cropley, V. L., 2021. Large-scale evidence for an association between peripheral inflammation and white matter free water in schizophrenia and healthy individuals. Schizophr. Bull. 47, 542–551. https://doi.org/10.1093/schbul/sbaa134.

Dietz, A.G., Goldman, S.A., Nedergaard, M., 2020. Glial cells in schizophrenia: a unified hypothesis. Lancet Psychiatry 7, 272–281. https://doi.org/10.1016/S2215-0366(19) 30302-5.

Erkol, C., Cohen, T., Chouinard, V.-A., Lewandowski, K.E., Du, F., Öngür, D., 2020. White matter measures and cognition in schizophrenia. Front. Psychiatry 11, 603. https://doi.org/10.3389/fpsyt.2020.00603.

Faizy, T.D., Thaler, C., Broocks, G., Flottmann, F., Leischner, H., Kniep, H., Nawabi, J., Schön, G., Stellmann, J.-P., Kemmling, A., Reddy, R., Heit, J.J., Fiehler, J., Kumar, D., Hanning, U., 2020. The myelin water fraction serves as a marker for age-related myelin alterations in the cerebral white matter – a multiparametric MRI aging study. Front. Neurosci. 14 https://doi.org/10.3389/fnins.2020.00136.

Febo, M., Perez, P.D., Ceballos-Diaz, C., Colon-Perez, L.M., Zeng, H., Ofori, E., Golde, T. E., Vaillancourt, D.E., Chakrabarty, P., 2020. Diffusion magnetic resonance imaging-derived free water detects neurodegenerative pattern induced by interferon-γ. Brain Struct. Funct. 225, 427–439. https://doi.org/10.1007/s00429-019-02017-1.

Flynn, S.W., Lang, D.J., Mackay, A.L., Goghari, V., Vavasour, I.M., Whittall, K.P., Smith, G.N., Arango, V., Mann, J.J., Dwork, A.J., Falkai, P., Honer, W.G., 2003. Abnormalities of myelination in schizophrenia detected in vivo with MRI, and post-mortem with analysis of oligodendrocyte proteins. Mol. Psychiatry 8, 811–820. https://doi.org/10.1038/sj.mp.4001337.

Fond, G., Lançon, C., Korchia, T., Auquier, P., Boyer, L., 2020. The role of inflammation in the treatment of schizophrenia. Front. Psychiatry 11. https://doi.org/10.3389/fpsyt.2020.00160.

Frydecka, D., Krzystek-Korpacka, M., Lubeiro, A., Stramecki, F., Stańczykiewicz, B., Beszłej, J.A., Piotrowski, P., Kotowicz, K., Szewczuk-Bogusławska, M., Pawlak-Adamska, E., Misiak, B., 2018. Profiling inflammatory signatures of schizophrenia: a cross-sectional and meta-analysis study. Brain Behav. Immun. 71, 28–36. https://doi.org/10.1016/j.bbi.2018.05.002.

Gangadin, S.S., Nasib, L.G., Sommer, I.E.C., Mandl, R.C.W., 2019. MRI investigation of immune dysregulation in schizophrenia. Curr. Opin. Psychiatry 32, 164–169. https://doi.org/10.1097/YCO.0000000000000498.

Godbout, J.P., Johnson, R.W., 2009. Age and neuroinflammation: a lifetime of psychoneuroimmune consequences. Immunol. Allergy Clin. N. Am. 29, 321–337. https://doi.org/10.1016/j.iac.2009.02.007.

Goldsmith, D.R., Rapaport, M.H., Miller, B.J., 2016. A meta-analysis of blood cytokine network alterations in psychiatric patients: comparisons between schizophrenia, bipolar disorder and depression. Mol. Psychiatry 21, 1696–1709. https://doi.org/10.1038/mp.2016.3.

Guo, J.Y., Lesh, T.A., Niendam, T.A., Ragland, J.D., Tully, L.M., Carter, C.S., 2020. Brain free water alterations in first-episode psychosis: a longitudinal analysis of diagnosis, course of illness, and medication effects. Psychol. Med. 1–10. https://doi.org/10.1017/S0033291719003969.

Gurholt, T.P., Haukvik, U.K., Lonning, V., Jönsson, E.G., Pasternak, O., Agartz, I., 2020. Microstructural white matter and links with subcortical structures in chronic schizophrenia: a free-water imaging approach. Front. Psychiatry 11, 56. https://doi.org/10.3389/fpsyt.2020.00056.

Harrison, N.A., Cooper, E., Dowell, N.G., Keramida, G., Voon, V., Critchley, H.D., Cercignani, M., 2015. Quantitative magnetization transfer imaging as a biomarker for effects of systemic inflammation on the brain. Biol. Psychiatry 78, 49–57. https://doi.org/10.1016/j.biopsych.2014.09.023.

Hegde, R.R., Kelly, S., Lutz, O., Guimond, S., Karayumak, S.C., Mike, L., Mesholam-Gately, R.I., Pasternak, O., Kubicki, M., Eack, S.M., Keshavan, M.S., 2020. Association of white matter microstructure and extracellular free-water with cognitive performance in the early course of schizophrenia. Psychiatry Res. Neuroimaging 305, 111159. https://doi.org/10.1016/j.pscychresns.2020.111159.

Hidese, S., Ota, M., Matsuo, J., Ishida, I., Yokota, Y., Hattori, K., Yomogida, Y., Kunugi, H., 2020. Association between obesity and white matter microstructure impairments in patients with schizophrenia: a whole-brain magnetic resonance imaging study. Schizophr. Res. https://doi.org/10.1016/j.schres.2020.07.009.

Jenkinson, M., Bannister, P., Brady, M., Smith, S., 2002. Improved optimization for the robust and accurate linear registration and motion correction of brain images. NeuroImage 17, 825–841. https://doi.org/10.1016/s1053-8119(02)91132-8.

Jeppesen, R., Christensen, R.H.B., Pedersen, E.M.J., Nordentoft, M., Hjorthøj, C., Köhler-Forsberg, O., Benros, M.E., 2020. Efficacy and safety of anti-inflammatory agents in treatment of psychotic disorders – a comprehensive systematic review and meta-analysis. Brain Behav. Immun. 90, 364–380. https://doi.org/10.1016/j.bbi.2020.08.028.

Kay, S.R., Fiszbein, A., O.L.A, 1987. The positive and negative syndrome scale for schizophrenia. Schizophr. Bull. 13, 261–276. https://doi.org/10.1093/schbul/13.2.261.

Keefe, R.S.E., Goldberg, T.E., Harvey, P.D., Gold, J.M., Poe, M.P., Coughenour, L., 2004. The brief assessment of cognition in schizophrenia: reliability, sensitivity, and comparison with a standard neurocognitive battery. Schizophr. Res. 68, 283–297. https://doi.org/10.1016/j.schres.2003.09.011.

Kelly, S., Jahanshad, N., Zalesky, A., Kochunov, P., Agartz, I., Alloza, C., Andreassen, O. A., Arango, C., Banaj, N., Bouix, S., Bousman, C.A., Brouwer, R.M., Bruggemann, J., Bustillo, J., Cahn, W., Calhoun, V., Cannon, D., Carr, V., Catts, S., Chen, J., Chen, J.-x., Chen, X., Chiapponi, C., Cho, K.K., Ciullo, V., Corvin, A.S., Crespo-Facorro, B., Cropley, V., De Rossi, P., Diaz-Caneja, C.M., Dickie, E.W., Ehrlich, S., Fan, F.-M., Faskowitz, J., Fatouros-Bergman, H., Flyckt, L., Ford, J.M., Fouche, J.-P., Fukunaga, M., Gill, M., Glahn, D.C., Gollub, R., Goudzwaard, E.D., Guo, H., Gur, R. E., Gur, R.C., Gurholt, T.P., Hashimoto, R., Hatton, S.N., Henskens, F.A., Hibar, D.P., Hickie, I.B., Hong, L.E., Horacek, J., Howells, F.M., Hulshoff Pol, H.E., Hyde, C.L., Isaev, D., Jablensky, A., Jansen, P.R., Janssen, J., Jönsson, E.G., Jung, L.A., Kahn, R. S., Kikinis, Z., Liu, K., Klauser, P., Knöchel, C., Kubicki, M., Lagopoulos, J., Langen, C., Lawrie, S., Lenroot, R.K., Lim, K.O., Lopez-Jaramillo, C., Lyall, A., Magnotta, V., Mandl, R.C.W., Mathalon, D.H., McCarley, R.W., McCarthy-Jones, S., McDonald, C., McEwen, S., McIntosh, A., Melicher, T., Mesholam-Gately, R.I., Michie, P.T., Mowry, B., Mueller, B.A., Newell, D.T., O'Donnell, P., Oertel-Knöchel, V., Oestreich, L., Paciga, S.A., Pantelis, C., Pasternak, O., Pearlson, G., Pellicano, G.R., Pereira, A., Pineda Zapata, J., Piras, F., Potkin, S.G., Preda, A., Rasser, P.E., Roalf, D.R., Roiz, R., Roos, A., Rotenberg, D., Satterthwaite, T.D., Savadjiev, P., Schall, U., Scott, R.J., Seal, M.L., Seidman, L.J., Shannon Weickert, C., Whelan, C.D., Shenton, M.E., Kwon, J.S., Spalletta, G., Spaniel, F., Sprooten, E., Stäblein, M., Stein, D.J., Sundram, S., Tan, Y., Tan, S., Tang, S., Temmingh, H.S., Westlye, L.T., Tønnesen, S., Tordesillas-Gutierrez, D., Doan, N.T., Vaidya, J., van Haren, N.E.M., Vargas, C., Vecchio, D., Velakoulis, D., Voineskos, A., Voyvodic, J. Q., Wang, Z., Wan, P., Wei, D., Weickert, T.W., Whalley, H., White, T., Whitford, T. J., Wojcik, J.D., Xiang, H., Xie, Z., Yamamori, H., Yang, F., Yao, N., Zhang, G., Zhao, J., van Erp, T.G.M., Turner, J., Thompson, P.M., Donohoe, G., 2018. Widespread white matter microstructural differences in schizophrenia across 4322 individuals: results from the ENIGMA schizophrenia DTI working group. Mol. Psychiatry 23, 1261–1269. https://doi.org/10.1038/mp.2017.170.

Kochunov, P., Ganjgahi, H., Winkler, A., Kelly, S., Shukla, D.K., Du, X., Jahanshad, N., Rowland, L., Sampath, H., Patel, B., O'Donnell, P., Xie, Z., Paciga, S.A., Schubert, C. R., Chen, J., Zhang, G., Thompson, P.M., Nichols, T.E., Hong, L.E., 2016. Heterochronicity of white matter development and aging explains regional patient control differences in schizophrenia. Hum. Brain Mapp. 37, 4673–4688. https://doi.org/10.1002/hbm.23336.

Kolind, S.H., Mädler, B., Fischer, S., Li, D.K.B., MacKay, A.L., 2009. Myelin water imaging: implementation and development at 3.0T and comparison to 1.5T measurements. Magn. Reson. Med. 62, 106–115. https://doi.org/10.1002/mrm.21966.

Kraguljac, N.V., Anthony, T., Monroe, W.S., Skidmore, F.M., Morgan, C.J., White, D.M., Patel, N., Lahti, A.C., 2019. A longitudinal neurite and free water imaging study in patients with a schizophrenia spectrum disorder. Neuropsychopharmacology 44, 1932–1939. https://doi.org/10.1038/s41386-019-0427-3.

Kraguljac, N.V., Anthony, T., Morgan, C.J., Jindal, R.D., Burger, M.S., Lahti, A.C., 2020. White matter integrity, duration of untreated psychosis, and antipsychotic treatment response in medication-naïve first-episode psychosis patients. Mol. Psychiatry. https://doi.org/10.1038/s41380-020-0765-x.

Kubicki, M., Park, H., Westin, C.F., Nestor, P.G., Mulkern, R.V., Maier, S.E., Niznikiewicz, M., Connor, E.E., Levitt, J.J., Frumin, M., Kikinis, R., Jolesz, F.A., McCarley, R.W., Shenton, M.E., 2005. DTI and MTR abnormalities in schizophrenia: analysis of white matter integrity. NeuroImage 26, 1109–1118. https://doi.org/10.1016/j.neuroimage.2005.03.026.

Lang, D.J.M., Yip, E., MacKay, A.L., Thornton, A.E., Vila-Rodriguez, F., MacEwan, G.W., Kopala, L.C., Smith, G.N., Laule, C., MacRae, C.B., Honer, W.G., 2014. 48 echo T2 myelin imaging of white matter in first-episode schizophrenia: evidence for aberrant myelination. NeuroImage Clin. 6, 408–414. https://doi.org/10.1016/j.nicl.2014.10.006.

Lesh, T.A., Maddock, R.J., Howell, A., Wang, H., Tanase, C., Daniel Ragland, J., Niendam, T.A., Carter, C.S., 2019. Extracellular free water and glutathione in first-episode psychosis—a multimodal investigation of an inflammatory model for psychosis. Mol. Psychiatry 43. https://doi.org/10.1038/s41380-019-0428-y. S142-S142.

Lipp, I., Jones, D.K., Bells, S., Sgarlata, E., Foster, C., Stickland, R., Davidson, A.E., Tallantyre, E.C., Robertson, N.P., Wise, R.G., Tomassini, V., 2019. In: Comparing MRI Metrics to Quantify White Matter Microstructural Damage in Multiple Sclerosis, pp. 2917–2932. https://doi.org/10.1002/hbm.24568.

Lyall, A.E., Pasternak, O., Robinson, D.G., Newell, D., Trampush, J.W., Gallego, J.A., Fava, M., Malhotra, A.K., Karlsgodt, K.H., Kubicki, M., Szeszko, P.R., A.E, L., O, P., D. G, R., D, N., J.W, T., J.A, G., M, F., A.K, M., K.H, K., M., K., P.R, S., Lyall, A.E., Pasternak, O., Robinson, D.G., Newell, D., Trampush, J.W., Gallego, J.A., Fava, M., Malhotra, A.K., Karlsgodt, K.H., Kubicki, M., Szeszko, P.R., 2017. Greater extracellular free-water in first-episode psychosis predicts better neurocognitive functioning. Mol. Psychiatry 23, 701–707. https://doi.org/10.1038/mp.2017.43.

MacKay, A.L., Laule, C., 2016. Magnetic resonance of myelin water: an in vivo marker for myelin. Brain Plast. 2, 71–91. https://doi.org/10.3233/BPL-160033.

Mandl, R.C.W., Pasternak, O., Cahn, W., Kubicki, M., Kahn, R.S.R.S., Shenton, M.E., Hulshoff Pol, H.E., 2015. Comparing free water imaging and magnetization transfer measurements in schizophrenia. Schizophr. Res. 161, 126–132. https://doi.org/10.1016/j.schres.2014.09.046.

Marques, T.R., Ashok, A.H., Pillinger, T., Veronese, M., Turkheimer, F.E., Dazzan, P., Sommer, I.E.C., Howes, O.D., 2019. Neuroinflammation in schizophrenia: meta-analysis of in vivo microglial imaging studies. Psychol. Med. 49, 2186–2196. https://doi.org/10.1017/S0033291718003057.

Najjar, S., Pearlman, D.M., 2015. Neuroinflammation and white matter pathology in schizophrenia: systematic review. Schizophr. Res. 161, 102–112. https://doi.org/10.1016/j.schres.2014.04.041.

Nazeri, A., Chakravarty, M.M., Felsky, D., Lobaugh, N.J., Rajji, T.K., Mulsant, B.H., Voineskos, A.N., 2013. Alterations of superficial white matter in schizophrenia and relationship to cognitive performance. Neuropsychopharmacology 38, 1954–1962. https://doi.org/10.1038/npp.2013.93.

Oestreich, L.K.L., Lyall, A.E., Pasternak, O., Kikinis, Z., Newell, D.T., Savadjiev, P., Bouix, S., Shenton, M.E., Kubicki, M., Whitford, T.J., McCarthy-Jones, S., 2017. Characterizing white matter changes in chronic schizophrenia: a free-water imaging multi-site study. Schizophr. Res. 189, 153–161. https://doi.org/10.1016/j.schres.2017.02.006.

Pasternak, O., Westin, C.-F.C.-F., Bouix, S., Seidman, L.J., Goldstein, J.M., Woo, T.-U., Petryshen, T.L., Mesholam-Gately, R.I.R.I., McCarley, R.W.R., Kikinis, R., Shenton, M.E., Kubicki, M., 2012. Excessive extracellular volume reveals a neurodegenerative pattern in schizophrenia onset. J. Neurosci. 32, 17365–17372. https://doi.org/10.1523/JNEUROSCI.2904-12.2012.

Pasternak, O., Kubicki, M., Shenton, M.E., 2016. In vivo imaging of neuroinflammation in schizophrenia. Schizophr. Res. 173, 200–212. https://doi.org/10.1016/j.schres.2015.05.034.

Plavén-Sigray, P., Matheson, G.J., Coughlin, J.M., Hafizi, S., Laurikainen, H., Ottoy, J., De Picker, L., Rusjan, P., Hietala, J., Howes, O.D., Mizrahi, R., Morrens, M., Pomper, M.G., Cervenka, S., 2021. Meta-analysis of the glial marker TSPO in psychosis revisited: reconciling inconclusive findings of patient-control differences. Biol. Psychiatry 89, e5–e8. https://doi.org/10.1016/j.biopsych.2020.05.028.

Pollak, T.A., Drndarski, S., Stone, J.M., David, A.S., McGuire, P., Abbott, N.J., 2018. The blood–brain barrier in psychosis. Lancet Psychiatry 5, 79–92. https://doi.org/10.1016/S2215-0366(17)30293-6.

Rodrigue, A.L., Knowles, E.E., Mollon, J., Mathias, S.R., Koenis, M.M., Peralta, J.M., Leandro, A.C., Fox, P.T., Sprooten, E., Kochunov, P., Olvera, R.L., Duggirala, R., Almasy, L., Curran, J.E., Blangero, J., Glahn, D.C., 2019. Evidence for genetic correlation between human cerebral white matter microstructure and inflammation. Hum. Brain Mapp. 40, 4180–4191. https://doi.org/10.1002/hbm.24694.

Shahab, S., Stefanik, L., Foussias, G., Lai, M.-C., Anderson, K.K., Voineskos, A.N., 2018. Sex and diffusion tensor imaging of white matter in schizophrenia: a systematic review plus meta-analysis of the corpus callosum. Schizophr. Bull. 44, 203–221. https://doi.org/10.1093/schbul/sbx049.

Smith, S.M., 2002. Fast robust automated brain extraction. Hum. Brain Mapp. 17, 143–155. https://doi.org/10.1002/hbm.10062.

Smith, S.M., Jenkinson, M., Johansen-Berg, H., Rueckert, D., Nichols, T.E., Mackay, C.E., Watkins, K.E., Ciccarelli, O., Cader, M.Z., Matthews, P.M., Behrens, T.E.J., 2006. Tract-based spatial statistics: voxelwise analysis of multi-subject diffusion data. NeuroImage 31, 1487–1505. https://doi.org/10.1016/j.neuroimage.2006.02.024.

Sneeboer, M.A.M., van der Doef, T., Litjens, M., Psy, N.B.B., Melief, J., Hol, E.M., Kahn, R.S., de Witte, L.D., 2020. Microglial activation in schizophrenia: is translocator 18 kDa protein (TSPO) the right marker? Schizophr. Res. 215, 167–172. https://doi.org/10.1016/j.schres.2019.10.045.

Snijders, G.J.L.J., Zuiden, W., Sneeboer, M.A.M., Berdenis van Berlekom, A., Geest, A.T., Schnieder, T., MacIntyre, D.J.M., Hol, E.M., Kahn, R.S., Witte, L.D., 2021. A loss of mature microglial markers without immune activation in schizophrenia. Glia, glia.23962. https://doi.org/10.1002/glia.23962.

Sommer, I.E.C., Gangadin, S.S., de Witte, L.D., Koops, S., van Baal, C., Bahn, S., Drexhage, H., van Haren, N.E.M., Veling, W., Bruggeman, R., Martens, P., Wiersma, S., Veerman, S.R.T., Grootens, K.P., van Beveren, N., Kahn, R.S., Begemann, M.J.H., 2021. Simvastatin augmentation for patients with early-phase schizophrenia-spectrum disorders: a double-blind, randomized placebo-controlled trial. Schizophr. Bull. https://doi.org/10.1093/schbul/sbab010.

Spangaro, M., Mazza, E., Poletti, S., Cavallaro, R., Benedetti, F., 2018. Obesity influences white matter integrity in schizophrenia. Psychoneuroendocrinology 97, 135–142. https://doi.org/10.1016/j.psyneuen.2018.07.017.

Szeszko, P.R., Robinson, D.G., Ikuta, T., Peters, B.D., Gallego, J.A., Kane, J., Malhotra, A. K., 2014. White matter changes associated with antipsychotic treatment in first-episode psychosis. Neuropsychopharmacology 39, 1324–1331. https://doi.org/10.1038/npp.2013.288.

Trépanier, M.O., Hopperton, K.E., Mizrahi, R., Mechawar, N., Bazinet, R.P., 2016. Postmortem evidence of cerebral inflammation in schizophrenia: a systematic review. Mol. Psychiatry 21, 1009–1026. https://doi.org/10.1038/mp.2016.90.

van Kesteren, C.F.M.G., Gremmels, H., de Witte, L.D., Hol, E.M., Van Gool, A.R., Falkai, P.G., Kahn, R.S., Sommer, I.E.C., 2017. Immune involvement in the pathogenesis of schizophrenia: a meta-analysis on postmortem brain studies. Transl. Psychiatry 7, e1075. https://doi.org/10.1038/tp.2017.4.

Vanes, L.D., Mouchlianitis, E., Wood, T.C., Shergill, S.S., 2018. White matter changes in treatment refractory schizophrenia: does cognitive control and myelination matter? NeuroImage Clin. 18, 186–191. https://doi.org/10.1016/j.nicl.2018.01.010.

Vanes, L.D., Mouchlianitis, E., Barry, E., Patel, K., Wong, K., Shergill, S.S., 2019. Cognitive correlates of abnormal myelination in psychosis. Sci. Rep. 9, 1–9. https://doi.org/10.1038/s41598-019-41679-z.

Wang, Z., Li, P., Chi, D., Wu, T., Mei, Z., Cui, G., 2017. Association between C-reactive protein and risk of schizophrenia: an updated meta-analysis. Oncotarget 8, 75445–75454. https://doi.org/10.18632/oncotarget.17995.

Weiser, M., Zamora, D., Levi, L., Nastas, I., Gonen, I., Radu, P., Matei, V., Nacu, A., Boronin, L., Davidson, M., Davis, J., 2020. Adjunctive aspirin vs placebo in patients with schizophrenia: results of two randomized controlled trials. Schizophr. Bull. 47 (4), 1077–1087.

Wheeler, A.L., Voineskos, A.N., 2014. A review of structural neuroimaging in schizophrenia: from connectivity to connectomics. Front. Hum. Neurosci. 8, 653. https://doi.org/10.3389/fnhum.2014.00653.

Winkler, A.M., Ridgway, G.R., Webster, M.A., Smith, S.M., Nichols, T.E., 2014. Permutation inference for the general linear model. NeuroImage 92, 381–397. https://doi.org/10.1016/j.neuroimage.2014.01.060.

Wood, T.C., 2018. QUIT: QUantitative imaging tools. J. Open Source Softw. 3, 656. https://doi.org/10.21105/joss.00656.

Zhou, Y., Liu, J., Driesen, N., Womer, F., Chen, K., Wang, Y., Jiang, X., Zhou, Q., Bai, C., Wang, D., Tang, Y., Wang, F., 2017. White matter integrity in genetic high-risk individuals and first-episode schizophrenia patients: similarities and disassociations. Biomed. Res. Int. 2017, 1–9. https://doi.org/10.1155/2017/3107845.